O-373

J. Chem. Thermodynamics **1990**, 22, 979–990

Heat capacity and thermodynamic properties of deuterated ammonium hexafluorophosphate ND_4PF_6 from 5.8 K to 347 K [a]

JANE E. CALLANAN,

Centre for Chemical Technology, National Institute of Standards and Technology, Boulder, CO 80303, U.S.A.

RON D. WEIR,[b]

Department of Chemistry and Chemical Engineering, Royal Military College of Canada, Kingston, Ontario K7K 5LO, Canada

and EDGAR F. WESTRUM, JR.

Department of Chemistry, University of Michigan, Ann Arbor, MI 48109-1055, U.S.A.

(Received 20 March 1990; in final form 29 May 1990)

The heat capacity of deuterated ammonium hexafluorophosphate ND_4PF_6 was measured from 5.8 K to 347 K by adiabatic calorimetry. Two λ-shaped anomalies were found in the curve for heat capacity against temperature. The upper anomaly reached a peak $C_{p,m} \approx 600 \cdot R$ at (194.4 ± 0.05) K with $\Delta_{trs}S^\circ_m = (1.013 \pm 0.016) \cdot R$ ($R = 8.3145\ J \cdot K^{-1} \cdot mol^{-1}$). The lower anomaly is also λ-shaped but is gradual, continuous, and reaches its maximum $C_{p,m} = 19.2 \cdot R$ at (137.5 ± 1.0) K with $\Delta_{trs}S^\circ_m = (0.562 \pm 0.011) \cdot R$. Both anomalies are characteristic of order-disorder transitions. Smoothed values of the standard thermodynamic quantities are tabulated up to 350 K.

1. Introduction

Interest in rotational motion of ammonium ions within ammonium crystals continues to generate both theoretical and experimental studies. In ammonium salts where polyatomic anions are present, the distribution of the anionic charge over several atoms weakens the electrostatic attraction between any of these atoms and a hydrogen of an NH_4^+ ion. As a result, the barrier to rotation of the ammonium ion in

[a] Partial contribution of the National Institute of Standards and Technology (formerly U.S. National Bureau of Standards). Not subject to copyright.

[b] To whom correspondence should be sent.

such salts is expected to be low. In some ammonium crystals, phase transitions, which affect rotational freedom, are absent, and the rotational barrier is more or less independent of temperature. In such cases, if the anion carries a single charge, the NH_4^+ ion is likely to behave as a molecule trapped in a spherical cell (much like a clathrate), where it may rotate with little or no restriction. However, virtually no solids are known where the ammonium ions rotate with the same freedom in the solid as in the gas, but there are some solids in which the rotational barrier is very low. These include NH_4PF_6 at 0.8 $kJ \cdot mol^{-1}$,[1] NH_4ClO_4 at < 4 $kJ \cdot mol^{-1}$,[2 6] and ND_4ClO_4 at 4 $kJ \cdot mol^{-1}$.[7]

The anticipated low barrier in NH_4PF_6 instigated the heat-capacity study by Staveley *et al.*,[8] but the finding of a λ-type transition, which reached a maximum value of heat capacity at 191.8 K, and an anomaly which peaked around 131 K, ruled out their reaching definitive conclusions about the rotational or torsional movements of the NH_4^+ ions. However, they were able to conclude that the upper transition was an order-disorder process, which subsequently[9] was shown to result from changes in the rotational states of the PF_6^- ion. Albert and Gutowsky[9] concluded from their n.m.r. work that the lower anomaly was also an order-disorder transition in the dynamic state of the NH_4^+ ions, similar to that in NH_4Cl and NH_4Br. Unfortunately, the crystal structure of NH_4PF_6 is known only above 191.8 K for the high-temperature phase, which is highly symmetrical with space group Fm3m (No. 225 O_h^5), four formula units in the face-centred cubic cell, and a cell constant $a = 0.792$ nm at room temperature.[10,11] The six PF_6^- ions are arranged around the NH_4^+ ions in a highly symmetrical way.

In NH_4PF_6, the spin exchange between the protons and ^{19}F nuclei may play a role in the spin-lattice relaxation and this cross-relaxation can be lowered by replacing the protons by deuterons. This effect was studied by Niemalä and Tuohi[12] and Albert and Gutowsky,[9] who measured spin-lattice relaxation times of the deuterons and ^{19}F nuclei in solid ND_4PF_6. Both studies suggested two phase transitions in the deuterated ND_4PF_6 at about 132 K to 134 K and at 192 K to 195 K. Thermodynamic values for these transitions and heat capacities of the deuterated ND_4PF_6 have not been published, and a knowledge of these properties should help in understanding the mechanisms of molecular rotations and phase transitions. Therefore, we have undertaken the study by adiabatic calorimetry as part of our ongoing work with ammonium salts.

2. Experimental

The sample of ND_4PF_6 was prepared from NH_4PF_6, supplied as a commercial sample with a minimum purity of 99.5 mass per cent. About 37 g was dissolved in 150 cm^3 of D_2O (99.8 moles per cent minimum isotopic purity) contained in a dish made of (ethene + tetrafluoroethene) copolymer which was chemically inert to the reagents. Most of the NH_4PF_6 dissolved at 294 K; to ensure complete dissolution, the mixture was warmed to 335 K. Upon recrystallization, a partially deuterated product was obtained. This procedure, carried out in a dry atmosphere, was repeated four times, whereupon the crystalline ND_4PF_6 product amounted to 19 g. To

remove most of the D_2O trapped as fluid inclusions in the crystals of ND_4PF_6 upon recrystallization, the ND_4PF_6 salt was dried under vacuum in a desiccator, where the sample was kept at 302 K for 48 h and then at 295 K for 144 h during which time pumping was continuous. A t.g.a. was done on 10 mg to 20 mg samples removed at intervals.

The Guinier–de Wolff X-ray diffraction patterns of our powdered ND_4PF_6 sample were found to be in excellent agreement with the standard pattern for this compound: No. 7-254 as determined by the Joint Committee for Powder Diffraction Standards.[10] The structure was found to be face-centred cubic at room temperature with $a = (0.79232 \pm 0.00004)$ nm. The structure of our starting material NH_4PF_6 was also in agreement with the standard pattern for the compound, a face-centred cubic structure with $a = 0.790$ nm.

As a check for D_2O trapped within our "dried" sample of ND_4PF_6, the final t.g.a. was done on a 20 mg portion of the sample which was to be subsequently loaded into the calorimeter. On heating to 411 K, a mass loss of 0.15 per cent occurred. Above 413 K, decomposition began slowly. A platinum resistance thermometer was used in the t.g.a. instrument to measure temperature and was calibrated at the ice point and the fixed points of the Curie transition in Alumel at 422.5 K, in nickel at 631.2 K, and in Trafoperm (97 mass per cent of Fe + 3 mass per cent of Si) at 1018.8 K. The estimated precisions were ± 2 K and $\pm 1 \times 10^{-6}$ g.

The molar heat capacity $C_{p,m}$ was measured from 5.8 K to 347 K by adiabatic calorimetry in the Mark XIII adiabatic cryostat, which is an upgraded version of the Mark II cryostat described previously.[13] A guard shield was incorporated to surround the adiabatic shield. A Leeds and Northrup capsule-type platinum resistance thermometer (laboratory designation A-5) was used for temperature measurements. The thermometer was calibrated at the U.S. National Bureau of Standards (N.B.S.) against the IPTS-1948 (as revised in 1960)[14] for temperatures above 90 K, against the N.B.S. provisional scale from 10 K to 90 K, and by the technique of McCrackin and Chang[15] below 10 K. These calibrations are judged to reproduce thermodynamic temperatures to within 0.03 K between 10 K and 90 K and within 0.04 K above 90 K.[16] Measurements of mass, current, potential difference, and time were based upon calibrations done at N.B.S. The acquisition of heat capacities from about 5 K to 350 K was computer assisted.[17,18] The computer was programmed for a series of determinations. During the drift periods, both the calorimeter temperature and the first and second derivatives of temperature with time were recorded to establish the equilibrium temperature of the calorimeter before and after the energy input. While the calorimeter heater was on, the heater current and potential, the duration of the heating current and potential, and the duration of the heating interval were obtained. Also recorded were the apparent heat capacity of the system including the calorimeter, heater, thermometer, and sample.

A gold-plated copper calorimeter (laboratory designation W-62) with four internal vertical vanes and a central entrant well for (heater + thermometer) was loaded with ND_4PF_6 within a dry box. The sample had been ground to fine particles in a mortar and pestle. Following the loading, the calorimeter was evacuated and pumping was continued for several hours to ensure that no free D_2O remained within the sample.

Helium gas was then added to the vessel to a pressure of about 3.3 kPa at 300 K so as to facilitate thermal equilibration. The vessel was then sealed by means of an annealed gold gasket tightly pressed on to the stainless-steel knife edge of the calorimeter top by means of a screw closure about 5 mm in diameter.

Buoyancy corrections were calculated on the basis of a crystallographic density of 2.230 $g \cdot cm^{-3}$ derived from the unit-cell edge of our sample. The mass of the ND_4PF_6 was 18.91315 g ($\triangleq$0.1132342 mol, based on its molar mass of 167.0269 $g \cdot mol^{-1}$ from IUPAC 1983 relative atomic masses).

The thermal history of the ND_4PF_6 is represented by the following linear array. The arrows indicate cooling or heating, which corresponds to acquisition of heat-capacity results.

$$300\ \text{K} \xrightarrow{20\,\text{h}} 5\ \text{K} \xrightarrow[\text{Series I}]{9\,\text{h}} 72\ \text{K} \xrightarrow{11\,\text{h}} 66\ \text{K} \xrightarrow[\text{Series II}]{5\,\text{h}} 127\ \text{K} \xrightarrow[\text{Series III}]{13\,\text{h}} 244\ \text{K} \xrightarrow[\text{Series IV}]{8\,\text{h}} 349\ \text{K}$$

$$\xrightarrow{9\,\text{h}} 114\ \text{K} \xrightarrow[\text{Series V}]{3\,\text{h}} 217\ \text{K} \xrightarrow{12\,\text{h}} 134\ \text{K} \xrightarrow[\text{Series VI}]{2\,\text{h}} 140\ \text{K} \xrightarrow{1\,\text{h}} 194\ \text{K} \xrightarrow[\text{Series VII}]{4\,\text{h}} 206\ \text{K}.$$

3. Results

The experimental molar heat capacities for ND_4PF_6 are given in table 1. Except for points in the region of the λ-shaped anomalies, the standard errors in our heat-capacity results decrease from about 1 per cent at 10 K to less than 0.15 per cent at temperatures above 30 K. The heat capacity of our sample represented about 51 per cent to nearly 100 per cent of the measured total heat capacity, and the maximum occurred at the peak of the heat capacity at $T \approx 194$ K.

A plot of $C_{p,m}/R$ against T from 6 K to 347 K is shown in figure 1, where one λ-shaped transition peaks with very high values around 194 K, and a second, but smaller, anomaly reaches its maximum around 137 K. By making our heat-capacity measurements with sufficiently short heating periods, the temperature where the heat capacities reached their maximum was found to be (194.4 ± 0.05) K and (137.5 ± 1) K for the upper and lower transitions, respectively. Three passes were made through the region of the two anomalies (see the thermal history above, Series III, V, VI, and VII), and reproducible heat capacities resulted. The details of the two peaks are given in figure 2. The reproducibility of our measurements of the enthalpy and entropy changes through these regions is presented in tables 2 and 3. No rise in the heat capacity was evident around 270 K to 275 K where fusion of any D_2O trapped as inclusions in the crystals of ND_4PF_6 would be expected to occur. However, 0.15 mass per cent of trapped D_2O would have been expected to give about a 9 per cent increase in the heat capacity over the 5 K interval of a single run. This was not detected. It is, therefore, presumed that the volatile contaminant was adsorbed water removed in the desiccation of the sample at room temperature prior to measurement.

Special care was exercised with the particle size and thermal history of our ND_4PF_6 sample in view of the phenomenon of hysteresis encountered by other workers. Morphee and Staveley[19] discovered that heat capacities of NH_4PF_6 and $RbPF_6$,[8] as well as $(NH_4)_2SnCl_6$, K_2SnCl_6, and Rb_2SnCl_6,[19] were diminished by

TABLE 1. Experimental molar heat capacity of ND_4PF_6 ($M = 167.0269\ g \cdot mol^{-1}$; $R = 8.31451\ J \cdot K^{-1} \cdot mol^{-1}$)

T/K	$C_{p,m}/R$	T/K	$C_{p,m}/R$	T/K	$C_{p,m}/R$	T/K	$C_{p,m}/R$
Series I		Series II		195.44	18.16	Series V	
5.77	0.0405	69.67	9.836	196.83	16.95	$\Delta_{trs}H_m$ Detns A. B	
6.70	0.06253	74.51	10.51	198.95	16.91	116.87	15.53
7.62	0.09678	79.34	11.17	201.89	17.03	161.00	16.73
8.48	0.1544	84.22	11.85	205.26	17.16	202.71	17.23
9.32	0.1954	89.12	12.48	209.37	17.30	208.30	17.47
9.98	0.2576	94.07	13.03	214.16	17.55	213.83	17.70
10.60	0.3281	99.03	13.63	219.17	17.69	Series VI	
11.54	0.4251	104.04	14.10	224.35	18.01	134.55	18.78
12.54	0.5450	109.05	14.71	229.73	18.26	135.62	19.02
13.62	0.6982	114.08	15.22	235.42	18.46	136.70	19.19
14.78	0.8809	119.13	15.81	241.12	18.67	137.76	19.22
16.05	1.091	124.17	16.50	Series IV		138.83	19.11
17.44	1.336	Series III		246.80	18.84	139.89	18.77
18.98	1.605	129.20	17.39	252.56	19.02	Series VII	
20.54	1.897	134.22	18.71	258.22	19.23	193.95	517.6
22.11	2.215	139.19	19.12	263.88	19.45	193.99	632.5
23.89	2.562	144.22	17.34	269.54	19.68	194.04	415.7
25.86	2.932	149.42	16.49	275.19	19.98	194.17	89.66
27.83	3.285	154.65	16.36	280.87	20.11	194.64	18.65
30.00	3.718	159.85	16.51	286.53	20.25	195.32	17.17
32.37	4.130	164.87	16.86	292.18	20.51	196.02	17.07
34.89	4.592	170.02	17.20	297.83	20.56	196.71	16.96
37.52	5.027	174.97	17.71	303.48	20.83	197.41	16.95
40.35	5.515	179.20	18.22	309.12	21.02	198.11	17.01
43.17	6.013	182.34	18.69	314.76	21.21	198.99	17.05
46.18	6.475	185.07	19.19	320.40	21.37	200.06	17.11
49.49	7.038	187.75	19.82	326.04	21.59	201.45	17.18
52.84	7.537	190.37	20.80	331.69	21.77	203.18	17.21
56.67	8.115	192.77	27.15	337.35	21.86	204.91	17.33
60.96	8.670	194.00	277.2	343.00	22.07		
65.30	9.301	194.45	376.6	347.36	22.18		
69.26	9.835	194.67	63.94				

TABLE 2. Summary of the thermophysical quantities through the lower transition for ND_4PF_6 ($R = 8.31451\ J \cdot K^{-1} \cdot mol^{-1}$). T_1 and T_2 denote the beginning and ending temperatures, respectively, for two enthalpy determinations (Series V) through the transition (including determination A of ΔH)

	$\frac{T_1}{K}$	$\frac{T_2}{K}$	$\frac{\Delta_{T_1}^{T_2}H_m^\circ}{R \cdot K}$	$\frac{\Delta_{87K}^{155K}H_m^\circ}{R \cdot K}$	$\frac{\Delta_{87K}^{155K}S_m}{R}$
	114.256	155.467	718.8	107.0	
Graphical integration:				1072.2 ± 2.0[a]	8.940 ± 0.003
Lattice contribution:				999.2 ± 2.0[a]	8.378 ± 0.008
$\Delta_{trs}H_m^\circ/(R \cdot K)$:				74.1 ± 2.0	
$\Delta_{trs}S_m^\circ/R$:					0.562 ± 0.011

[a] Error due to the uncertainty in the position of the lattice heat-capacity curve through the region of the anomaly.

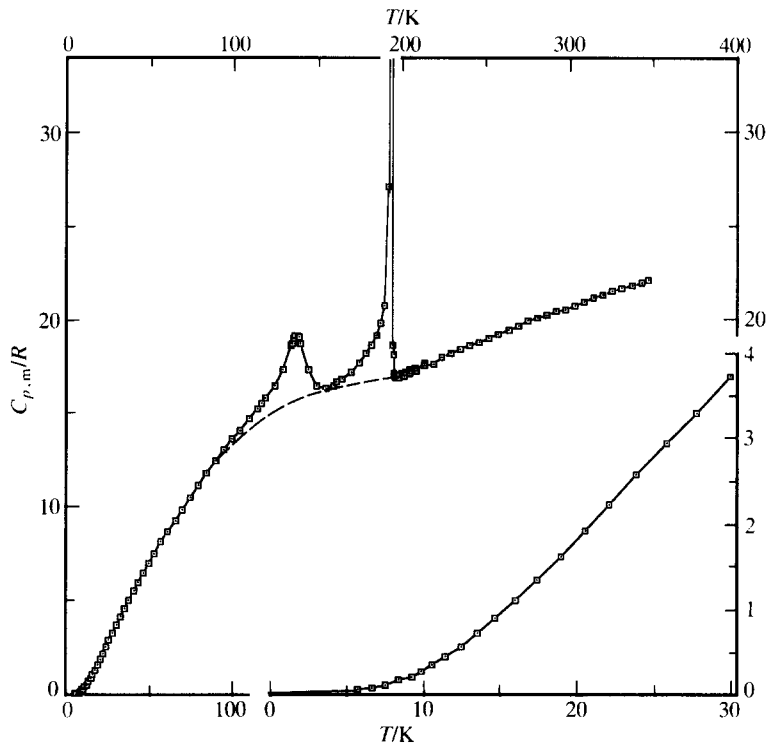

FIGURE 1. Experimental molar heat capacities at constant pressure $C_{p,m}$ plotted against temperature for deuterated ammonium hexafluorophosphate ND_4PF_6.

repeated cooling to liquid-nitrogen or liquid-air temperatures. Reproducible results were obtained only after repeated cooling. For their specimen of NH_4PF_6, they found that one cooling to liquid-air temperature was sufficient to result in reproducible heat capacities. The curve through their first values of $C_{p,m}$ diverged

TABLE 3. Summary of the thermophysical quantities through the upper transition for ND_4PF_6 ($R = 8.31451\ J \cdot K^{-1} \cdot mol^{-1}$). T_1 and T_2 denote the beginning and ending temperatures, respectively, for the enthalpy determinations through the transition (including determination B of ΔH)

	$\frac{T_1}{K}$	$\frac{T_2}{K}$	$\frac{\Delta_{T_1}^{T_2} H_m^\circ}{R \cdot K}$	$\frac{\Delta_{155\,K}^{200\,K} H_m^\circ}{R \cdot K}$	$\frac{\Delta_{155\,K}^{200\,K} S_m^\circ}{R}$
	155.468	216.569	1199.7	930.5	
Graphical integration:				941.3 ± 11.0^a	5.246 ± 0.008
Lattice contribution:				749.6 ± 2.0^b	4.233 ± 0.008
$\Delta_{trs} H_m^\circ/(R \cdot K)$:				180.9 ± 2.0	
$\Delta_{trs} S_m^\circ/R$:					1.013 ± 0.016

[a] Error due to the uncertainty in the position of the experimental heat-capacity curve through the peak of the transition.

[b] Error due to the uncertainty in the position of the lattice heat-capacity curve through the region of the transition.

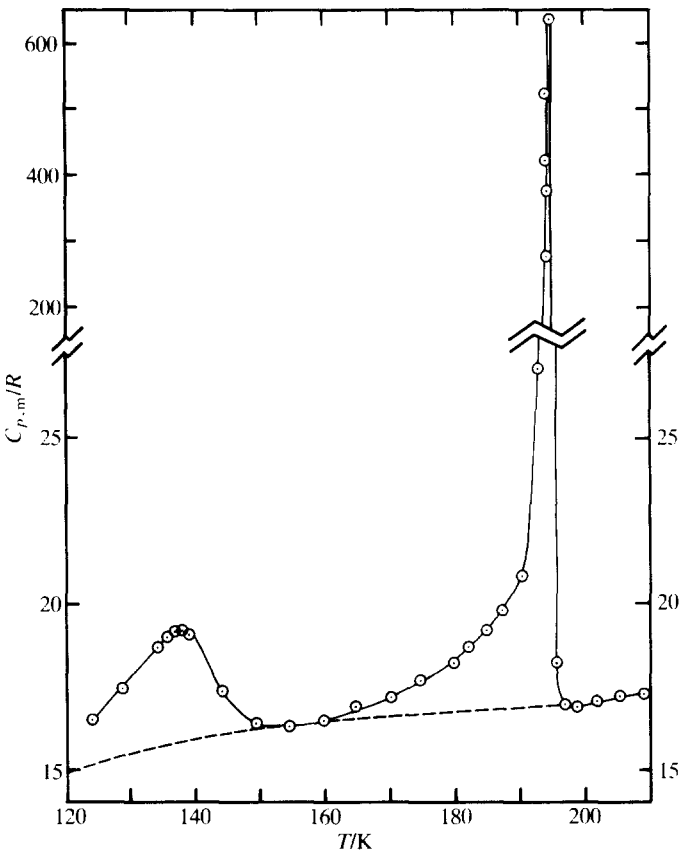

FIGURE 2. Experimental molar heat capacities at constant pressure $C_{p,m}$ plotted against temperature through the region of transitions from 120 K to 210 K for deuterated ammonium hexafluorophosphate ND_4PF_6.

gradually from the points taken as the final values, and resulted in a 3 per cent lowering of $C_{p,m}$ at 300 K. Miller and Gutowsky[20] found in their n.m.r. study that the temperature dependence of the fluorine resonance in KPF_6 and $RbPF_6$ depended upon particle size and previous physical treatment. Reproducible results were obtained on samples in the form of fine powders. Those that were crystalline before the first cooling showed hysteresis, and the cooling-warming process served to break up the crystallites into small particles and powders, thereby removing the effects of hysteresis. Our sample of ND_4PF_6 was ground to fine particles before it was loaded into the calorimeter and it was then cooled directly from 300 K to 5 K in 20 h when the measurements began. No differences are apparent between the $C_{p,m}$ values in our seven series of runs.

Integration of the smoothed values for heat capacity and for the enthalpy and entropy increments through the anomalies yielded the thermodynamic functions. Values of $C_{p,m}/R$ and the derived functions are presented at selected temperatures in

TABLE 4. Standard molar thermodynamic functions for ND_4PF_6

$M = 167.0269\ g \cdot mol^{-1}$, $p^\circ = 101.325\ kPa$, $R = 8.31451\ J \cdot K^{-1} \cdot mol^{-1}$, $\Phi_m^\circ \stackrel{def}{=} \Delta_0^T S_m^\circ - \Delta_0^T H_m^\circ / T$

T K	$C_{p,m}^\circ / R$	$\Delta_0^T S_m^\circ / R$	$\Delta_0^T H_m^\circ / R \cdot K$	Φ_m° / R	T K	$C_{p,m}^\circ / R$	$\Delta_0^T S_m^\circ / R$	$\Delta_0^T H_m^\circ / R \cdot K$	Φ_m° / R
0	0	0	0	0	170	17.24	20.18	1827.9	9.429
5	(0.0262)	(0.0124)	(0.0399)	(0.0044)		(16.55)	(19.60)	(1751.8)	(9.292)
10	0.260	0.0840	0.625	0.022	180	18.35	21.20	2005.4	10.06
15	0.907	0.299	3.38	0.073		(16.65)	(20.55)	(1917.8)	(9.891)
20	1.800	0.679	10.10	0.174	190	20.64	22.21	2193.3	10.70
25	2.750	1.184	21.57	0.324		(16.85)	(21.45)	(2085.3)	(10.48)
30	3.700	1.767	37.61	0.514	193	30.00	22.58	2263.2	10.85
35	4.600	2.397	58.11	0.737		(16.89)	(21.72)	(2135.9)	(10.65)
40	5.445	3.059	82.97	0.985	194	500.00	23.03	2350.7	10.91
45	6.295	3.749	112.3	1.253		(16.91)	(21.80)	(2152.8)	(10.71)
50	7.122	4.455	145.9	1.537	195	17.70	23.45	2433.3	10.97
55	7.865	5.168	183.3	1.835		(16.91)	(21.89)	(2169.7)	(10.76)
60	8.555	5.882	224.4	2.143	200	17.03	23.88	2518.5	11.29
65	9.245	6.594	268.9	2.458		(17.03)	(22.32)	(2254.5)	(11.05)
70	9.810	7.304	316.8	2.779	210	17.38	24.72	2690.5	11.91
75	10.57	8.010	368.0	3.104		(17.38)	(23.16)	(2426.5)	(11.60)
80	11.27	8.715	422.6	3.432	220	17.80	25.54	2866.4	12.51
85	11.95	9.418	480.6	3.764		(17.80)	(23.98)	(2602.4)	(12.15)
90	12.57	10.12	541.9	4.098	230	18.23	26.34	3046.5	13.10
	[a](12.52)	(10.12)	(541.8)	(4.098)		(18.23)	(24.78)	(2782.5)	(12.68)
95	13.15	10.81	606.2	4.433	240	18.61	27.13	3230.7	13.67
	(13.00)	(10.81)	(605.6)	(4.433)		(18.61)	(25.56)	(2966.7)	(13.20)
100	13.73	11.50	673.4	4.769	250	18.93	27.89	3418.4	14.22
	(13.40)	(11.48)	(671.5)	(4.768)		(18.93)	(26.33)	(3154.4)	(13.71)
105	14.19	12.18	743.2	5.106	260	19.29	28.64	3609.4	14.76
	(13.85)	(12.15)	(739.6)	(5.104)		(19.29)	(27.08)	(3345.5)	(14.21)
110	14.74	12.86	815.5	5.443	270	19.72	29.38	3804.4	15.29
	(14.24)	(12.79)	(808.8)	(5.439)		(19.72)	(27.81)	(3540.5)	(14.70)
115	15.33	13.53	890.6	5.780	280	20.10	30.10	4003.5	15.80
	(14.61)	(13.43)	(880.9)	(5.773)		(20.10)	(28.54)	(3739.5)	(15.18)
120	15.93	14.19	968.7	6.117	290	20.42	30.81	4206.2	16.31
	(14.92)	(14.06)	(954.7)	(6.105)		(20.42)	(29.25)	(3942.2)	(15.65)
125	16.62	14.85	1050.1	6.453	300	20.70	31.51	4411.7	16.80
	(15.19)	(14.68)	(1030.0)	(6.436)		(20.70)	(29.94)	(4147.7)	(16.12)
130	17.56	15.52	1135.4	6.789	310	21.05	32.19	4620.4	17.29
	(15.43)	(15.28)	(1106.5)	(6.764)		(21.05)	(30.63)	(4356.4)	(16.58)
135	18.89	16.21	1226.5	7.125	320	21.40	32.87	4832.6	17.77
	(15.65)	(15.86)	(1184.2)	(7.090)		(21.40)	(31.30)	(4568.6)	(17.03)
140	18.77	16.90	1321.9	7.462	330	21.71	33.53	5048.1	18.23
	(15.86)	(16.44)	(1263.0)	(7.414)		(21.71)	(31.97)	(4784.1)	(17.47)
145	17.20	17.53	1411.5	7.798	340	21.99	34.18	5266.7	18.69
	(16.05)	(17.00)	(1342.8)	(7.735)		(21.99)	(32.62)	(5002.6)	(17.90)
150	16.44	18.10	1495.4	8.133	350	22.22	34.82	5487.8	19.15
	(16.22)	(17.54)	(1423.5)	(8.053)		(22.22)	(33.26)	(5223.8)	(18.33)
160	16.53	19.16	1659.4	8.789	298.15	20.65	31.38	4373.4	16.71
	(16.44)	(18.60)	(1586.9)	(8.679)		±0.02	±0.03	±6.0	±0.02

[a] Quantities in parentheses represent the values taken on the lattice curve.

table 4. The corresponding values for the lattice heat capacities beneath the two anomalies, drawn by smooth extrapolation of the curves, are shown in parentheses and plotted in figure 1 as the dashed line. This smooth lattice curve touches the solid line at 155 K. In assessing the enthalpy and entropy changes associated with these two anomalies, the "extra" heat capacity above 155 K was taken to belong to the upper anomaly, and that below 155 K was assigned to the lower-temperature anomaly. The heat capacities of ND_4PF_6 below 6 K were obtained by fitting our experimental values below 20 K to the limiting form of the Debye equation, with a plot of $C_{p,m}/T^3$ against T^2 and extrapolation to $T \rightarrow 0$; see equation (3) below.

4. Discussion

The quantity measured calorimetrically is $C_{sat,m}$, the heat capacity of the solid or liquid in equilibrium with its saturated vapour. For solid ND_4PF_6, $C_{sat,m}$ is virtually identical with $C_{p,m}$ as the right-hand side of equation (1) is negligible.

$$C_{sat,m} - C_{p,m} = (\partial p/\partial T)_{sat}\{(\partial H/\partial p)_T - V_m\}. \tag{1}$$

However, analysis of heat-capacity results requires $C_{V,m}$, which is related to $C_{p,m}$ *via*

$$C_{p,m} - C_{V,m} = V_m T\alpha^2/\kappa_T, \tag{2}$$

where $\alpha = V_m^{-1}(\partial V_m/\partial T)_p$ is the isobaric expansivity, V_m is the molar volume, and $\kappa_T = -V_m^{-1}(\partial V_m/\partial p)_T$ is the isothermal compressibility. Values of α and κ_T are unavailable for ND_4PF_6 but, fortunately, at temperatures below 20 K, $(C_{p,m} - C_{V,m}) \approx 0$.

The heat capacity of an insulator at very low temperatures can be described by a power series of the form:

$$C_{V,m} = aT^3 + bT^5 + cT^7 + \cdots, \tag{3}$$

in which the coefficients a, b, and c are directly related to the corresponding power series for the frequency spectrum at low frequencies.[21] As $T \rightarrow 0$, the lattice heat capacity of the crystal should become equal to that of an elastic continuum and can be described by the Debye T^3 law:

$$C_{V,m} = aT^3, \tag{4}$$

$$\Theta_0^C = (12\pi^4 Lk/5a)^{1/3}, \tag{5}$$

where Θ_0^C is the Debye temperature derived from heat capacity and L is Avogadro's constant.

A useful plot, figure 3, for identifying any non-vibrational contributions to the heat capacity at low temperatures, is a graph of $C_{p,m}/T^3$ against T^2: see equation (3). In the region $36 < (T^2/K^2) < 400$ {*i.e.* $6 < (T/K) < 20$}, the graph of our experimental heat capacities for ND_4PF_6 resembles that for argon[22,23] and suggests that only lattice vibrations make significant contributions to the heat capacity in this temperature range. By extrapolating the points below $T^2 = 36\ K^2$ in figure 3 to intersect the a/R axis at $T^2 = 0$, we found $10^4 a/R = (1.850 \pm 0.150)\ K^{-3}$ or

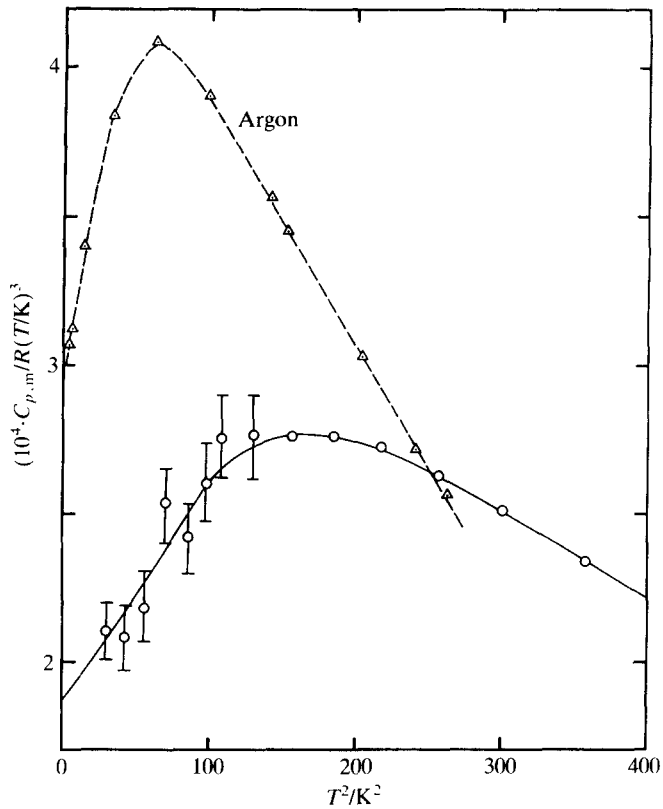

FIGURE 3. Experimental values of $C_{p,m}/RT^3$ plotted against T^2 for ND_4PF_6: ——, this work; – – –, argon.[19,20] The error bar represents 10 per cent.

$10^4 a = (15.4 \pm 1.2)\ J \cdot K^{-1} \cdot mol^{-1}$, which yields from equation (5) $\Theta_0^C = (108 \pm 2.6)$ K. This compares with 93.5 K for argon.

The temperatures and types of transition for MPF_6 as well as their $\Delta S_m/R$ values are compared in table 5 for $M = NH_4^+$, ND_4^+, K^+, and Rb^+. The potassium and rubidium salts show only one transition, whereas the ammoniated salts each possess two, presumably a result of some as yet undetermined influence of the ammonium

TABLE 5. Thermal and structural information on selected hexafluorophosphates, where λ denotes a lambda-type transition, and structure I is f.c.c. (Fm 3m)

Transition	T_{trs}/K	$\Delta_{trs}S_m/R$	References
NH_4PF_6(cr, III) = NH_4PF_6(cr, II)	131.3 (λ)	1.248	8
NH_4PF_6(cr, II) = NH_4PF_6(cr, I)	191.8 (λ)	1.122	10
ND_4PF_6(cr, III) = ND_4PF_6(cr, II)	137.5 (λ)	0.562	this work
ND_4PF_6(cr, II) = ND_4PF_6(cr, I)	194.4 (λ)	1.013	this work
$RbPF_6$(cr, II) = $RbPF_6$(cr, I)	207 (λ)	1.218	8, 24
KPF_6(cr, II) = KPF_6(cr, I)	273.9 (1st order)	3.46	8, 10

ions. This situation appears not to be comparable with the family of salts NH_4Cl and ND_4Cl, both of which show two transitions,[25-27] or to KCl and RbCl, which do not undergo phase transitions at $p = 0$, but do so at high pressures.[28] Outside the transition regions, the heat capacities of ND_4PF_6 and NH_4PF_6 are very similar. The $C_{p,m}/R$ for the ND_4^+ salt is greater by about 0.2 at 60 K, which increases gradually to about 0.4 at 300 K. An anomaly in this difference is apparent around 50 K, where the value peaks at 0.5. A proper analysis of the differences with the implications on librational motion is deferred.

It is unfortunate that the crystal structures of the low-temperature phases of NH_4PF_6 and ND_4PF_6 have not been published. The magnitude of the entropy change derived from our heat-capacity measurements suggests an order-disorder transition at 194.4 K for ND_4PF_6 with $\Delta_{trs}S^\circ_m = (1.013 \pm 0.016) \cdot R$ (compare $\ln 2 = 0.693$, $\ln 3 = 1.099$), which is what Staveley *et al.*[8] concluded for NH_4PF_6 at 191.8 K with $\Delta_{trs}S^\circ_m = 1.122 \cdot R$.

The lower transition in ND_4PF_6 is gradual, and although λ-shaped with $\Delta_{trs}S^\circ_m = (0.562 \pm 0.011) \cdot R$, the heat capacity is continuous with a broad peak which reaches its maximum at (137.5 ± 1.0) K. Its $\Delta_{trs}S^\circ_m$ value is smaller than that for NH_4PF_6, which may result from the somewhat arbitrary way in which the lattice curve is drawn beneath the transitions in both salts. Nevertheless, it is probable that the lower transitions in both NH_4PF_6 and ND_4PF_6 are associated with structural changes. Our heat-capacity results show the lower transition to occur from about 130 K to 145 K with the peak at (137.5 ± 1.0) K, rather higher than the (133 ± 1) K assigned to this transition by n.m.r. results.[12]

The n.m.r. studies of NH_4PF_6,[9] and ND_4PF_6,[12] led to the conclusion that in both salts a change occurred in the character of the PF_6 reorientations at the upper transition even though the PF_6^- is able to reorient rapidly above and below the transition. In both n.m.r. studies, the lower transition was found to have very little effect on the reorientational motion of the PF_6^-, ND_4^+, or NH_4^+ ions. The spin-lattice relaxation time T_1 for D^+, H^+, or $^{19}F^-$ was changed only slightly upon passing through the lower transition, which makes it impossible to conclude that this transition arises solely from the orientation of NH_4^+ or ND_4^+. A similar result was found in the proton T_1 measurements in NH_4Cl, NH_4Br, and NH_4I,[29] although the corresponding transitions in these salts occur at higher temperatures of 242.5 K,[30,31] 235.1 K,[32] and 231.0 K,[33] respectively. Niemelä and Tuohi[12] found for ND_4PF_6 at the lower transition that the activation energies for reorientational motion of both ND_4^+ and PF_6^- above this gradual transition were lower than those below the region. They concluded that this may be indicative of a structural change, which is consistent with our findings from heat capacity. There is a need for the determination of the structures of both the low-temperature phases of NH_4PF_6 and ND_4PF_6. Kearley *et al.*[34] note that they have determined the structure of ND_4PF_6 at 4 K by powder diffraction, but the manuscript to which they refer as having been submitted for publication in 1986 has apparently not appeared.

We thank Dr R. D. Heyding for determining the crystal structure of our sample, Mr J. Irving for running the t.g.a., and Ms T. Schefter for her help in the integrations for tables 2 to 4. One of us (R.D.W.) thanks the Department of National Defence (Canada) for financial support.

REFERENCES

1. Brajovic, V.; Boutin, H.; Safford, G. J.; Palevsky, H. *J. Phys. Chem. Solids* **1963,** 24, 617.
2. Rush, J. J.; Taylor, T. I.; Havens, W. W. *J. Chem. Phys.* **1962,** 37, 234.
3. Rush, J. J.; Taylor, T. I. *J. Phys. Chem.* **1964,** 68, 2534.
4. Leung, P. S.; Taylor, T. I.; Havens, W. W. *J. Chem. Phys.* **1968,** 48, 4912.
5. Riehl, J. W.; Wang, R.; Bernard, H. W. *J. Chem. Phys.* **1973,** 58, 508.
6. Prask, H. J.; Trevino, S. F.; Rush, J. J. *J. Chem. Phys.* **1975,** 62, 4156.
7. Bastow, T. J.; Brown, R. J. C.; Segel, S. L. *J. Chem. Phys.* **1988,** 89, 1203.
8. Staveley, L. A. K.; Grey, N. R.; Layzell, M. J. *Z. Naturforsch.* **1963,** 18A, 148.
9. Albert, S.; Gutowsky, H. S. *J. Chem. Phys.* **1973,** 59, 3585.
10. Bode, H.; Clausen, H. *Z. Anorg. Allg. Chem.* **1951,** 265, 229.
11. Wyckoff, R. W. G. *Crystal Structures. Vol. 3.* Interscience: New York. **1965,** p. 327.
12. Niemelä, L.; Tuohi, J. *Ann. Univ. Turku* **1970,** Series AI, No. 137, 1.
13. Westrum, E. F., Jr.; Furukawa, G. T.; McCullough, J. P. *Experimental Thermodynamics. Vol. I.* McCullough, J. P.; Scott, D. W.: editors. Butterworths: London. **1968,** p. 133.
14. Stimson, H. F. *J. Res. Natl. Bur. Stand.* **1961,** 65A, 139.
15. McCrackin, F. L.; Chang, S. S. *Rev. Sci. Instrum.* **1975,** 46, 550.
16. Chirico, R. D.; Westrum, E. F., Jr. *J. Chem. Thermodynamics* **1980,** 12, 311.
17. Andrews, J. T. S.; Norton, P. A.; Westrum, E. F., Jr. *J. Chem. Thermodynamics* **1978,** 10, 949.
18. Westrum, E. F., Jr. *Proceedings NATO Advanced Study Institute on Thermochemistry, Viana do Castello, Portugal.* Ribeiro da Silva, M. A. V.: editor. Reidel: New York. **1984,** p. 745.
19. Morphee, R. G. S.; Staveley, L. A. K. *Nature* **1957,** 180, 1246.
20. Miller, G. R.; Gutowsky, H. S. *J. Chem. Phys.* **1963,** 39, 1983.
21. Barron, T. H. K.; Berg, W. T.; Morrison, J. A. *Proc. Roy. Soc. London* **1957,** A242, 478.
22. Beaumont, R. H.; Chihara, H.; Morrison, J. A. *Proc. Phys. Soc. London* **1961,** 78, 1462.
23. Finegold, L.; Phillips, N. E. *Phys. Rev.* **1969,** 177, 1383.
24. Cox, B. *J. Chem. Soc.* **1956,** 876.
25. Levy, H. A.; Peterson, S. W. *Phys. Rev.* **1952,** 86, 766.
26. Tokunaga, M.; Koyano, N. *J. Phys. Soc. Jpn.* **1968,** 24, 1407.
27. Boiko, A. A. *Sov. Phys. Crystallogr.* **1970,** 14, 539.
28. Pistorius, C. W. F. T. *J. Phys. Chem. Solids* **1964,** 25, 1477.
29. Gutowsky, H. S.; Pake, G. E.; Bersohn, R. *J. Chem. Phys.* **1954,** 22, 643.
30. Schwartz, P. *Phys. Rev.* **1971,** B4, 920.
31. Chihara, H.; Nakamura, M. *Bull. Chem. Soc. Jpn.* **1972,** 45, 133.
32. Sorai, M.; Suga, H.; Seki, S. *Bull. Chem. Soc. Jpn.* **1965,** 38, 1125.
33. Stephenson, C. C.; Landers, L. A.; Cole, A. G. *J. Chem. Phys.* **1952,** 20, 1044.
34. Kearley, G. J.; Cockcroft, J. K.; Fitch, A. N.; Fender, B. E. F. *J. Chem. Soc. Chem. Commun.* **1986,** 1738.